DETERMINATION OF THE INTRINSIC FRACTURE TOUGHNESS FROM THE COD ANALYSIS OF INDENTATION CRACKS IN SPARK PLASMA SINTERED 3Y-TZP REINFORCED WITH MWCNT

F. García Marro, R. Kiran Chintapalli, A. Mestra and M. Anglada

Dep. Ciencia de los Materiales y Ing. Metalúrgica, Universidad Politécnica de Cataluña
Av. Diagonal, 647, 08028 Barcelona, España
E-mail: fernando.garcia.marro@upc.edu

RESUMEN

El método de la indentación para medir la tenacidad de fractura ha sido ampliamente utilizado en materiales frágiles debido a su sencillez y a que puede realizarse en volúmenes pequeños de material. Especialmente en estos casos, las tenacidades de fractura obtenidas mediante el método de indentación pueden llegar a ser muy distintas de los valores reales obtenidos mediante métodos rigurosos basados en un conocimiento preciso de todos los parámetros que intervienen en la fractura. Esto ha llevado a desarrollar métodos que relacionan el perfil de la abertura de la grieta de indentación con la tenacidad intrínseca de fractura K_{I0}. En este trabajo se ha estudiado la cerámica 3Y-TZP y el material compuesto formado por 3Y-TZP y 2 % en volumen de nanotubos de carbono con paredes multicapa (MWCNT) ambos producidos por Spark Plasma Sintering (SPS). El método de análisis del COD permitió comprobar que la adición de este contenido de MWCNT no afecta prácticamente al COD medido experimentalmente y que la tenacidad intrínseca K_{I0} es por tanto muy similar para ambos materiales. Estas observaciones en principio no justifican las diferencias en tenacidad de fractura determinadas por el método clásico de tenacidad de fractura por indentación en los materiales estudiados.

ABSTRACT

The indentation method has been widely used to measure the fracture toughness in fragile materials due to its simplicity and that only needs of a small sample. However, it is well known that the fracture toughness values obtained by indentation methods can be substantially different from the values obtained from more rigorous methods which are based on a precise knowledge of all parameters involved in fracture. This situation has lead to the development of new methods that investigate the crack opening displacement (COD) and relate it to the intrinsic fracture toughness K_{I0}. In the present work, a 3Y-TZP ceramic has been studied together with a composite containing 2 % vol. of multiwall carbon nanotubes (MWCNT); both of which were produced by Spark Plasma Sintering (SPS). The COD method showed that the addition of MWCNTs did not effectively affect the COD and the intrinsic fracture toughness K_{I0} was thus very similar in both materials. These observations in principle do not justify the differences determined by the classical indentation fracture toughness method on the present materials.

PALABRAS CLAVE: Cerámicas, Resistencia, Biomateriales

1. INTRODUCTION

Tetragonal zirconia stabilised with 3 mol % yttria (3Y-TZP) is used in many structural applications due to its excellent mechanical properties, which are related to transformation toughening and to its sub-micrometric grain size. The tetragonal-to-monoclinic (t-m) phase transformation plays a fundamental role by shielding the crack from external stresses as the crack extends. This mechanism can give rise to relatively high fracture toughness and it depends on the grain size and the yttria content [1].

The t-m transformation may also be activated by water vapour; this produces a microcracked monoclinic layer on the exposed surface; this phenomenon is referred to as hydrothermal ageing or low temperature degradation (LTD) [2]. Resistance to LTD ageing in a TZP ceramic can be improved by reducing the grain size; however this would diminish the transformation toughening capability and thus the overall fracture toughness. Therefore, this strategy for avoiding LTD has limitations. On the other hand, there has been interest in the addition of carbon nanotubes to zirconia and alumina [3]-[6] because of apparent improvements in fracture toughness [7], [8]. It is believed [9] that designing a TZP-based composite with a small quantity of carbon nanotubes as re-enforcements would improve the toughness without affecting the resistance to LTD because of the toughening by crack bridging and the fine grain size of zirconia achieved in the composite.

Up to date, the effect of carbon nanotubes addition to zirconia is not clearly understood. Some studies about the incorporation of multi-walled carbon nanotubes (MWCNT) to 3Y-TZP report increases in fracture toughness [5], [10], [11] while others found no improvement at all [12], [13]. Garmendia *et al* [14] and Mazaheri *et al* [15] reported improved fracture toughness which they attributed to crack bridging and MWCNT pull-out mechanisms. On the contrary, Sun *et al* [13] reported that the formation of MWCNT agglomerates at grain boundaries and a weak bonding between MWCNT and zirconia are responsible for decreasing hardness and no improvement in other

properties. There are many reasons for this disparity of results in the literature. The processing of the composite is a critical step that is yet no fully well defined; additionally it is difficult to maintain the grain size of the ceramic matrix when the nanotubes are added, which obviously has a strong effect on fracture toughness. Finally, different authors use different methods to determine the fracture toughness.

A key step for processing such composites is the correct dispersion of the carbon nanotubes in the ceramic matrix. Several methods have been attempted to obtain a good dispersion [10], [12], [16]-[18]. High power ultrasonication of MWCNT´s immersed in dispersant is known to produce agglomerate-free carbon nanotubes [19]; however, the effectiveness of this pre-treating method depends strongly on dispersant properties. Inam *et al* [20] reported that dimethylformamide (DMF) is an effective dispersant in producing an agglomerate-free MWCNT solution. Colloidal processing based on heterocoagulation mechanism was also shown to be effective when the MWCNTs were pre-treated [16]. In this sense, Garmendia *et al* [10] found that partially coating the nanotubes with zirconia improved their dispersion in the zirconia matrix, which was attributed to the increased surface area of the nanotubes. Datye *et al* [5] observed that in-situ growth of MWCNTs directly on to zirconia particles by chemical vapour deposition resulted in good dispersion after final sintering. Most works involve different methods for sintering these composites. Ceramic composites containing carbon nanotubes are usually sintered in Ar or N_2 atmosphere and/or hot isostatic pressing [10], [12], [16] except a few using spark plasma sintering (SPS) [5], [11]. In most cases, the final density achieved by SPS is still low as compared to monolithic ceramics, which is probably the main reason for the adverse effect on mechanical properties observed.

In this work, we have studied 3Y-TZP together with a nanocomposite of 3Y-TZP containing 2 % vol. of multi-walled carbon nanotubes (MWCNT), both of which ceramics were successfully produced by SPS sintering. The aim was to study the effect of the addition of this small quantity of MWCNTs on the mechanical properties of 3Y-TZP zirconia. The indentation fracture toughness was determined and the crack opening displacement (COD) of the indentation cracks was measured. COD profiles for both materials were compared and analysed in order to detect the influence of MWCNTs.

2. EXPERIMENTAL

Commercially available zirconia powder (TZ-3YSB-E, Tosoh Co, Japan) stabilised with 3 % molar of yttria was mixed with 2 % vol. of multiwalled carbon nanotubes (MWCNT Graphistrength C100, Arkema). Nanotubes were initially dispersed in N, N dimethylforamamide (DMF) using ultrasonication for 2 hours. The zirconia powder was preheated at 750 ºC for 1 hr and then added to the solution. The resulting slurry was milled for 4 hrs using different sized zirconia balls (10-5-3 mm). The final slurry was collected into a stainless steel tray and dried on a hot plate at 70 ºC for 24 hr. Finally the powder was sieved using a mesh of 250 μm. As well as this powder, another powder was produced without nanotubes for determining the properties of the ceramic without MWCNTs.

The prepared powders were introduced in a graphite die and sintered by spark plasma sintering (SPS FCT HP D25I, FCT system GmBh). Samples were sintered at maximum temperature of 1350 ºC with a dwell time of 5 min, with heating and cooling rates of 100 ºC/min. When the temperature reached 650 ºC during heating, the die started to apply a uniaxial pressure of 50 MPa which was maintained during the sintering cycle until the temperature finally descended below 800 ºC. The vacuum pressure inside the chamber was maintained at 1 Torr; heating current and voltage were 1300 A and 5.8 V. The final specimens had a disc shape (2 mm thickness, 20 mm diam.). Two ceramics were produced which will be labelled as SPS0 and SPS2 containing 0% 2% vol. nanotubes content. All samples were ground and polished with colloidal silica until a mirror-like finishing was reached. X-ray diffraction with Cu-K_α radiation (Bruker AXS D8) showed only tetragonal phase for both composites produced. The density of the samples was measured by the Archimedes method and was over > 99 % of the corresponding theoretical density. Microscopic observations of the prepared powders and fracture surfaces of the sintered samples were done by Scanning Electron Microscopy (SEM) revealing a grain size of 0.16 μm.

Vickers hardness (HV) was determined by 9.81 N indentation; additional indentations with a 98.1 N load were done to produce indentation cracks. In order to compare the results for indentation fracture toughness with those available in the literature, the indentation fracture toughness was determined with the expression of Anstis *et al* [21]:

$$K_{IC} = 0.016(E/H)^{1/2} P c^{-3/2} \qquad (1)$$

here c is the crack length measured from the centre of the indentation imprint, E is the elastic modulus and $H=P/2a^2$ is the hardness calculated from the indentation load P and the imprint half diagonal, a (see Figure 1).

Table 1: Mechanical properties of the samples.

Sample	***HV1*** **(GPa)**	K_{IC} (MPa√m)	***E*** **(GPa)**	H_{Berk} **(GPa)**
SPS0	14.9	3.9 ± 0.1	221 ± 3	16.1 ± 0.2
SPS2	13.3	4.5 ± 0.1	234 ± 4	15.3 ± 0.9

Contact hardness (H_{Berk}) and elastic modulus (E) were determined by nanoindentation (MTS Nanoindenter XP equipped with a CSM module) using the method of Oliver and Pharr [22]. Nanoindentation was performed

with a Berkovich diamond tip and a load of 630 mN under a constant deformation rate of 0.05 s^{-1}. Arrays of 4 by 4 indentations were carried out in each material; about 1200 data points (load, displacement, stiffness and time) were collected for each indentation. Table 1 shows the nanoindentation results together with other mechanical properties of the produced specimens.

Atomic force microscopy in tapping mode (AFM Dimension Veeco Inc) was used to determine the crack opening displacement (COD) of indentation cracks. A complete analysis of the COD profiles of Vickers indentation cracks in the absence of any extrinsic toughening mechanism has been carried out by Fett *et al* [23]; this expression can be approximated as [24]:

$$\delta_{app}(x)=\frac{K_{I0}\sqrt{a}}{E'}\left(\sqrt{\frac{8}{\pi}}(x/a)^{1/2}+A_1(x/a)^{3/2}+A_2(x/a)^{5/2}\right) \quad (2)$$

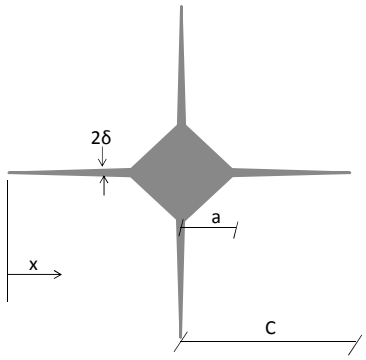

Figure 1: Scheme of an indentation crack.

Here, the coefficients A_1 and A_2 depend only on the ratio c/a, E' is the elastic modulus and K_{I0} is the crack tip fracture toughness. According to those authors, this expression describes correctly the COD profile in the range $1.4 \le c/a \le 3$. In the present case, the ratio c/a has been always confined between 2.2 and 2.4, so that equation (2) can be safely applied as far as the material does not present additional extrinsic toughening mechanisms. In the materials studied here, in principle, the measured COD δ_{meas} should be influenced by the contribution to shielding of transformation toughening and by bridging by the nanotubes in the composite, among other possible additional mechanisms of toughening, so that equation (2) might not describe δ_{meas}, unless the contribution of toughening mechanisms to δ_{meas} were negligible. One exception to these limitations is in the limit of $x \to 0$ when equation (2) is still valid giving the Irwin parabola from which the intrinsic fracture toughness can be determined (even in the presence of extrinsic toughening mechanisms):

$$\delta(x) \approx \frac{K_{I0}}{E'}\sqrt{\frac{8x}{\pi}} \quad ; \; x \to 0 \qquad (3)$$

3. RESULTS

AFM pictures of the crack profiles were analysed and the crack opening displacements for SPS2 and SPS0 were measured (Figure 2).

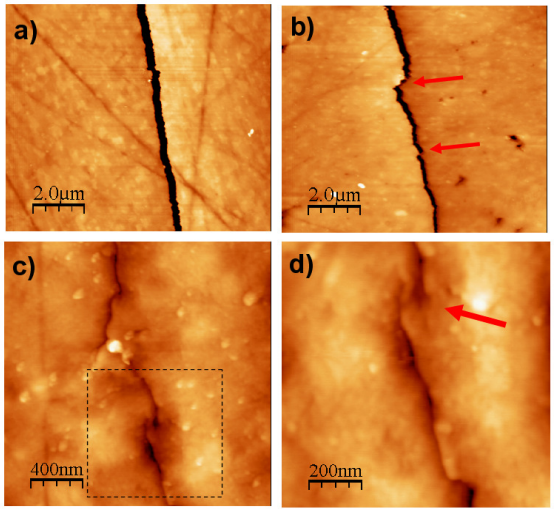

Figure 2: AFM images of indentation cracks: a) SPS0, b) SPS2; c) SPS2, close to the crack tip, d) enlargement of the bridge visible in c).

The indentation cracks were also observed by FE-SEM and the images were analysed to measure their COD. The COD profile of each sample was measured from both the FE-SEM and the AFM images, Figure 3 represents these profiles. For each sample (SPS0 and SPS2), two profiles are shown corresponding to the determination by AFM or FE-SEM. It can be appreciated how the COD profiles determined by AFM microscopy were slightly larger as those obtained by FE-SEM.

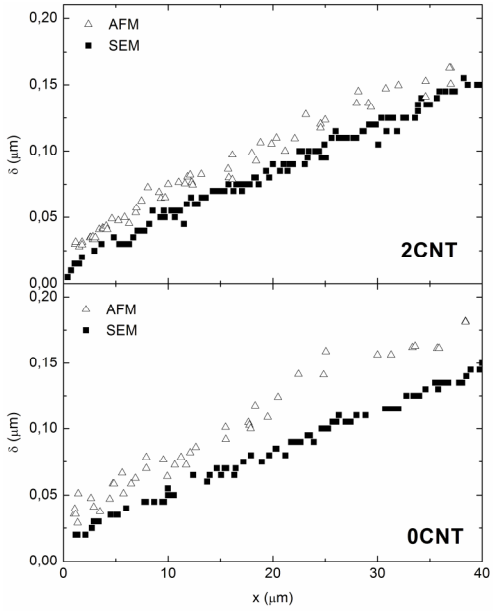

Figure 3: COD profiles for indentation cracks in samples SPS0 and SPS2. For each sample, the profile is shown as determined by AFM or FE-SEM microscopy.

The reason for this difference is that the images obtained by AFM are topological (Figure 2) and more difficult to analyze than the plain images obtained by FE-SEM, which reveal the crack width more clearly (see for example Figure 6). Because of this, the COD measured

by FE-SEM was that chosen to determine the intrinsic fracture toughness. It can be also appreciated that independently of the microscopy technique used, the COD profile is very similar for the samples with and without MWCNTs. This is surprising considering that the sample containing nanotubes showed shorter indentation cracks (see indentation fracture toughness in Table 1). The COD measured by FE-SEM on SP2 and SP0 are compared in Figure 4. It is clear that independently of the mechanisms of toughening in each material, the COD has practically identical values with and without MWCNT.

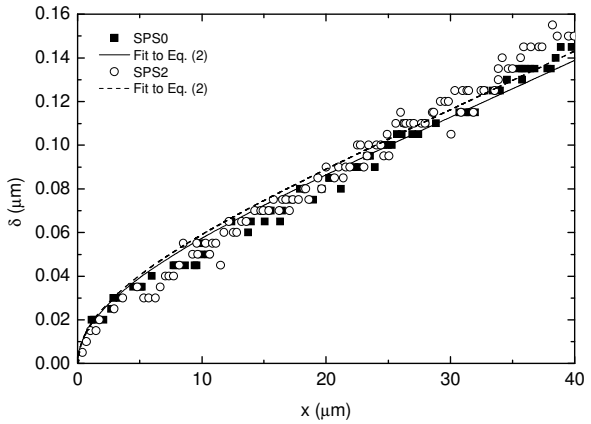

Fig. 4: COD profiles as determined by SEM for indentation cracks in SPS0 and SPS2

The crack tip fracture toughness was then determined from these COD profiles obtained by FE-SEM. A small region 10 μm close to the crack tip was analyzed, and it was considered that $E'=E/(1-\nu^2)$ in order to fit the Irwin parabola (equation (3)) to the profiles on both samples. This fitting is shown in Figure 5. The Irwin parabola for SPS0 and the composite SPS2 yielded 2.5 and 2.4 MPa√m, respectively Regarding the fitting of the COD by equation (3) there is some discrepancy in the literature whether the parameter E' to be used is for plane strain ($E'=E/(1-\nu^2)$) or plane stress ($E'=E$). The fitting of equation (3) was carried out by using the plane strain value. If the plane stress value is used, there is about a 10% decrease in the measured crack tip fracture toughness.

Both ceramics SPS0 and SPS2 showed grain crack bridging near the crack tip (see for example the AFM images in Figure 3). Additionally, further examination of SPS2 clearly revealed nanotubes across the fracture gap of the indentation crack (Figure 6). SPS2 also presented slightly more irregular crack paths as compared to the material without nanotubes (Figure 3). However no nanotubes pulling out could be observed on the fracture surfaces.

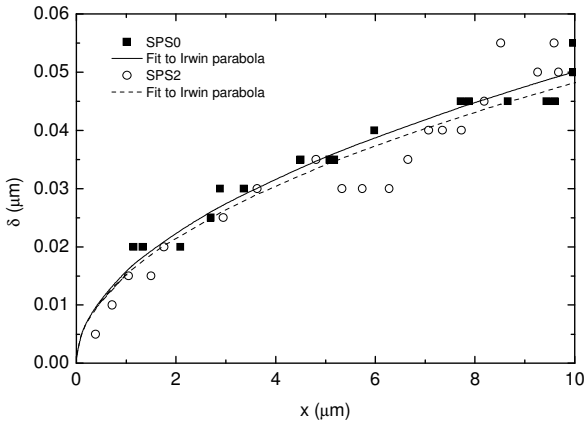

Figure 5: Fitting of the COD profiles as determined by FE-SEM for indentation cracks in SPS0 and SPS2, in a region very close to the crack tip to the Irwin parabola.

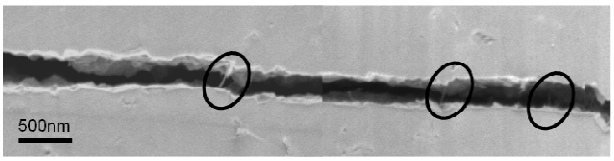

Figure 6: FE-SEM micrographs of indentation cracks in SPS2. Carbon nanotubes can be appreciated across the fracture gap (indicated with circles).

4. DISCUSSION

Examination of fracture surfaces showed no clear evidence of the presence of holes that could be left by pullout MWCNT from their matrix socket during fracture. Neither protruding sections of the nanotubes have been observed. Therefore, any hole or protruding section should be very small and this would be consistent with a small influence of toughening mechanisms such as fibre pull out.

The effect of crack bridging forces between the crack faces induced by MWCNT is important close to the crack tip. In materials with bridging stresses, the R-curve is represented by:

$$K_R = K_{I0} - K_{Br} \qquad (4)$$

Where K_{I0} is the intrinsic fracture toughness and the bridging contribution can be calculated as:

$$K_{Br} = \int_0^c h(x)\sigma_{Br}(x)dx \qquad (5)$$

Here, $h(x)$ is a weight function and $\sigma_{Br}(x)$ represents the bridging stress distribution along the crack. Typically, the bridging stress is maximum (σ_{max}) very close to the crack tip (x=0) and decreases with the distance to the tip. Expressions for the function $h(x)$ can be found in the literature for the case of a semi-circular crack (see Fett *et al* [25] eq. 13-15). In order to simplify the calculation for $\sigma_{Br}(x)$ we shall use an exponentially decreasing bridging stress relation,

$$\sigma_{Br} = \sigma_0 \exp(-\delta/\delta_0) \qquad (6)$$

Here δ represents the COD and σ_0 and δ_0 are constants. In this simple expression, δ_0 represents a threshold crack opening displacement value over which bridging is irrelevant. This type of function has been found to describe the grain bridging behaviour of silicon nitride with comparatively much larger grains than in 3Y-TZP and by taking typical parameters of σ_0 = -180 MPa and δ_0 = 0.25 μm [26]. If we are only interested in the contribution to crack bridging of the MWCNTs located very close to the crack tip, we can use the near-tip solution for δ described by the Irwin parabola (equation (3)) which holds true for $x << c$. The calculation was made by taking several values of δ_0 together with two typical values of σ_0. As the values of δ used in the equation of the integral are only valid very close to the crack tip only the contribution from the region where the Irwin parabola has been fitted is taken into consideration (x = 10 μm). In this region the maximum value of δ is about 0.05 μm (see Figure 4) so that for $\delta_0 > 0.05$ μm the bridging stress is slowly decreasing from the maximum value of σ_0, while for $\delta_0 << 0.05$ μm the bridging stress decreases rapidly from the maximum value of σ_0, at the crack tip.

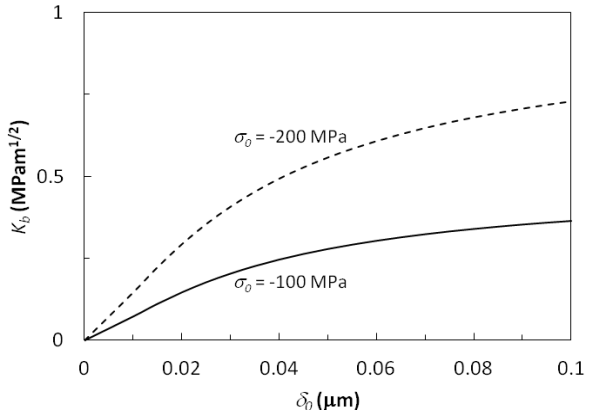

Fig. 7 Contribution of bridging stresses on a 10 μm region close to the crack tip, assuming two typical values of σ_0. This contribution was calculated for different possible δ_0 values.

From Figure 7, it is clear that crack bridging from the region close to the crack tip to fracture toughness will depend very much on the parameters used for of σ_0 and δ_0. If δ_0 was large this will mean the stress $\sigma_{Br}(x)$ will be close to the maximum and the corresponding increase in K_b is relatively high, but we have not observed changes in COD for SPS0 and SPS2. Therefore either σ_0, is very small (small bridging stresses because of easy debonding between MWCNT and matrix) or δ_0 is very small (less than about 0.02 μm) so that bridging stresses are only important at this small distance from the crack tip. In this case the corresponding very small increase in fracture toughness would be compatible with the present measurements of COD in SPS0 and SPS2. Therefore bridging stresses in the system studied here should be either very small or act only at very short distances from the crack tip.

The relationship between fracture toughness and COD is only valid in the region close to the crack tip. In case the increase in fracture toughness observed by the indentation method in the nanocomposites is a real effect, it should be associated to other mechanisms of toughening which do not induce changes in the crack opening displacement.

5. CONCLUSSIONS

The main conclusions are summarized as follows:

- The addition of 2 % vol. MWCNT to a 3Y-TZP matrix had the effect of reducing the length of indentation cracks on the ceramic. The only substantial difference between both materials is the presence of some nanotubes bridging the crack.
- The nanocomposite showed a slightly smaller hardness as determined by 1 kg Vickers indentation and by Berkovich nanoindentation.
- The COD profiles of indentation cracks yielded similar values for matrix and nanocomposite as well as similar intrinsic fracture toughness.

ACKNOWLEDGEMENTS

The authors gratefully acknowledge the financial support from the Ministerio de Ciencia e Innovación (MICINN) of Spain through project MAT2008-03398 and the partial grant given to F. G. Marro. The l financial support to the research group given by the Generalitat de Catalunya is also acknowledged (2009SGR01285). The authors are very grateful to Emilio Pique for making the nanoindentation measurements.

REFERENCES

[1] Richard H.J. Hannink, Patrick M. Kelly, Barry C. Muddle, *Transformation toughening in zirconia-containing ceramics*, J. Am. Ceram. Soc., 83 [3], pp. 461-487, 2000.

[2] Chevalier, J.; Laurent, G.; Sylvain, D. *Low-temperature degradation of zirconia and implications for biomedical implants*, Annu. Rev. Mater. Res. 37, pp. 1–32, 2007.

[3] Shi S-L., Liang J., *Effect of Multiwall carbon nanotubes on electrical and dielectric properties of yttria-stabilized zirconia ceramic*, J. Am. Ceram. Soc., 89[11], pp. 3533-3535, 2006.

[4] Dusza J., Blugan G., Morgiel J., *Hot pressed and spark plasma sintered zirconia/carbon nanofiber composites,* J. Eur. Ceram. Soc., 29(15), pp. 3177-3184, 2009.

[5] Datye A., Wu K.-H., Gomes G., *Synthesis, microstructure and mechanical properties of yttria stabilized zirconia (3YTZP)-multiwall nanotube (MWNTs) nanocomposite by direct in-situ growth of MWNTs on zirconia particles*, Composites Science and Technology, 70(14), pp. 2086-2092, 2010.

[6] Inam F., Yan H., Peijs T., Reece M.J. *The sintering and grain growth behaviour of ceramic–carbon nanotube nanocomposites,* Composites

Science and Technology, 70(6), pp. 947-952, 2010.
[7] Peigney A. *Tougher ceramics with nanotubes*, Nature materials, 2, pp. 15-16, 2002.
[8] Guo-Dong Zhan and Amiya K. Mukherjee. *Carbon nanotube reinforced alumina-Based ceramics with novel* mechanical, electrical and thermal properties, Int. J. Appl. Ceram. Technol., 1(2), pp.161-171, 2004.
[9] Garmendia N., Grandjean S., Chevalier J., *Zirconia–multiwall carbon nanotubes dense nano-composites with an unusual balance between crack and ageing resistance*, J. Eur. Ceram. Soc., 31(6), pp.1009-1014, 2011.
[10] Garmendia N., Santacruz I., Moreno R., Obieta I. *Zirconia-MWCNT nanocomposites for biomedical* applications obtained by colloidal processing. Journal of materials science. Materials in medicine, 21(5), pp.1445-51, 2010.
[11] Mazaheri M., Mari D., Schaller R., Bonnefont G., Fantozzi G., *Processing of yttria stabilized zirconia reinforced with multi-walled carbon nanotubes with attractive mechanical properties*, *J. Eur. Ceram. Soc*., 31(14), pp.2691-2698, 2011.
[12] Duszov A., Dusza J., Tomasek K., Blugan G., Kuebler J., *Microstructure and properties of carbon nanotube/zirconia composite*, J. Eur. Ceram. Soc., 28(5), pp. 1023-1027, 2008.
[13] Sun J., Gao L., Iwasa M., Nakayama T., Niihara K., *Failure investigation of carbon nanotube/3Y-TZP nanocomposites*, Ceramics International, 31(8), pp. 1131-1134, 2005.
[14] Garmendia N., Grandjean S., Chevalier J., *Zirconia–multiwall carbon nanotubes dense nano-composites with an unusual balance between crack and ageing resistance*, J. Eur. Ceram. Soc., 31(6), pp.1009-1014, 2011.
[15] Mazaheri M., Mari D., Hesabi Z.R., Schaller R., Fantozzi G., *Multi-walled carbon nanotube/nanostructured zirconia composites: Outstanding mechanical properties in a wide range of temperature*, Composites Science and Technology, 71(7), pp.939-945, 2011.
[16] Zhou J.P., Gong Q.M., Yuan K.Y., *The effects of multiwalled carbon nanotubes on the hot-pressed 3mol% yttria stabilized zirconia ceramics*, Materials Science and Engineering: A., 520(1-2), pp. 153-157, 2009.
[17] Duszova A., Dusza J., Tomasek K., *Zirconia / carbon nanofiber composite*, Scripta Materialia, 58, pp. 520-523, 2008.
[18] Zhan G-D., Kuntz J.D., Wan J., Mukherjee A.K. *Single-wall carbon nanotubes as attractive toughening agents in alumina-based nanocomposites*, Nature Materials, 2(1), pp. 38-42, 2003.
[19] Hilding J., Grulke E. A., Zhang Z. G., Lockwood F. *Dispersion of carbon nanotubes in liquids*, Journal of Dispersion Science and Technology, 24(1), pp. 1-41, 2003.
[20] Inam F., Yan H., Reece M.J., Peijs T. *Dimethylformamide: an effective dispersant for making ceramic–carbon nanotube composites.* Nanotechnology, 19(19), pp.195710 (5), 2008.
[21] Anstis G. R., Chantikul P., Lawn B. R., Marshall D. B., *A critical evaluation of indentation techniques for measuring, fracture toughness. I. Direct crack measurements*, J. Am. Ceram. Soc., 64, pp. 533–538, 1981.
[22] Oliver W. C., Pharr G. M., *Measurement of hardness and elastic modulus by instrumented indentation: Advances in understanding and refinements to methodology,* Journal of Materials Research, 19(1), pp. 3-20, 2004.
[23] Fett T., Kounga Njiwa A. B., Rödel J., *Crack opening displacements of Vickers indentation cracks*, Engineering Fracture Mechanics, 72, pp. 647–659, 2005.
[24] Schneider G. A., Fett T., *Computation of stress intensity factor and COD for submicron sized indentation cracks*, Journal of the Ceramic Society of Japan, 114, pp. 1044-1048, 2006.
[25] Fett T., Fünfschilling S., Hoffmann M. J., Oberacker R., *Different R-curves for two- and three-dimensional cracks*, Int. J. Fracture, 153, pp.153-159 2008.
[26] Fett T., Munz D., Kounga Nijwa A. B., Rödel J-, Quinn G. D. *Bridging stresses in sintered reaction-bonded Si_3N_4 from COD measurements*, J. Eur. Ceram. Soc., 25, pp.29-36 (2005).